Published in final edited form as:

ACS Biomater Sci Eng. 2018 September 10; 4(9): 3304–3316. doi:10.1021/acsbiomaterials.8b00491.

Probing fibroblast activation in response to extracellular cues with whole protein- or peptide-functionalized step-growth hydrogels

Megan E. Smithmyer, **Joseph B. Spohn**, **April M. Kloxin**

Department of Chemical and Biomolecular Engineering, University of Delaware, Newark, Delaware 19716, United States

Abstract

Synthetic hydrogels with well-defined mechanical properties have become invaluable tools for probing cell response to extracellular cues including matrix stiffness and integrin binding. These synthetic matrices are often decorated with either proteins or integrin-binding peptides to promote cell adhesion and to direct or probe cell behavior. For example, both collagen I-functionalized polyacrylamide and peptide-functionalized poly(ethylene glycol) hydrogels have been instrumental in elucidating the role of the elasticity or 'stiffness' of the matrix in promoting fibroblast activation in wound healing and fibrosis. However, the two methods of promoting integrin binding are not often directly compared in the same system, partly owing to differences in material designs, despite the potential differences in the way cells interact with whole proteins and protein mimetic peptides. We hypothesized that such a comparison could provide insight into the ways integrin binding affects fibroblast activation within commonly utilized *in vitro* cell culture models, and more broadly, to inform the design of materials to modulate fibroblast activation in studies of wound healing and disease. To enable this comparison, we developed a method to conjugate whole proteins to step-growth poly(ethylene glycol) (PEG) hydrogels and investigated fibroblast response to protein-peptide pairs: fibronectin and PHSRN$(G)_{10}$RGDS or collagen I and $(POG)_3$POGFOGER$(POG)_4$, which are important in matrix remodeling and relevant to fibroblast activation. With this approach, we observed that human pulmonary fibroblasts adopted a similar morphology on fibronectin and PHSRN$(G)_{10}$RGDS, although with a slight increase in the percentage of alpha smooth muscle actin (αSMA) expressing cells on PHSRN$(G)_{10}$RGDS. Interestingly, we observed that fibroblasts formed activated clusters on the collagen mimic $(POG)_3$POGFOGER$(POG)_4$ while exhibiting less activation on collagen I. This cell activation and clustering is reminiscent of fibroblast foci that are observed in lung fibrosis, suggesting the relevance of these well-defined polymer-peptide hydrogels for investigating fibrosis and decoupling biochemical and biophysical cues.

Keywords

hydrogel; collagen; synthetic extracellular matrix; fibroblast; fibrosis

akloxin@udel.edu.

Supporting Information. Figures S1 – S11

1. Introduction

Interactions between cells and their environment are known to play a crucial role in directing their function and fate in both wound healing and disease. For example, fibroblasts respond to changes in the extracellular matrix (ECM) during would healing by expressing alpha smooth muscle actin (αSMA) to enable contraction and secreting matrix metalloproteinases (MMPs) and new ECM proteins, including large amounts of collagen I, to remodel and repair the injured tissue.[1–3] This process of fibroblast activation in response to extracellular cues is mediated by integrins, cell surface protein dimers that interact with both the cytoskeleton of cells and specific amino acid sequences presented by ECM proteins and allow cells to sense and respond to the composition[4] and elasticity (or 'stiffness') of their environment.[5,6] How matrix composition influences fibroblast activation and persistence in wound healing and fibrosis remains an outstanding question in the field and is of importance for the design of approaches to both study and direct these complex processes.

Studies of cell-matrix interactions in well-defined material systems, like synthetic hydrogels, allow hypothesis testing with control of extracellular cues, such as integrin binding and material modulus, and probing relevant cell responses. In studies of fibroblast activation, synthetic hydrogel systems commonly use one of two methods for promoting integrin binding: the incorporation of whole proteins or integrin binding peptides. Traditionally, protein-functionalized polyacrylamide and peptide-functionalized poly(ethylene glycol) (PEG) hydrogels have been used as synthetic mimics of the ECM within *in vitro* culture models designed to control extracellular cues like stiffness and integrin binding and studying fibroblast activation.[7] Polyacrylamide hydrogels enable precise control of matrix mechanical properties over a wide range of moduli[8] and have been instrumental in investigating the ability of cells to sense and respond to the elasticity or 'stiffness' of their underlying matrix, [9,10] particularly for studies of fibroblast migration and activation.[5,11] Sulfo-SANPAH chemistry, amongst other methods, has been commonly used to attach whole ECM proteins, most often collagen I, to the surface of polyacrylamide hydrogels,[5,9,12,13] for promoting cell adhesion and integrin binding. For example, using polyacrylamide substrates presenting immobilized collagen I, matrices of higher stiffness were observed to promote fibroblast activation and inhibit the expression of anti-fibrogenetic cyclooxygenase-2 (COX-2) and prostaglandin E_2 (PGE_2), identifying these proteins as important parts of the mechanotransduction signaling cascade that leads to fibroblast activation.[5] While polyacrylamide-based cell culture systems continue to yield important discoveries, their translation for use in three-dimensional (3D) culture can be challenging owing to the limited cytocompatibility of the monomers and polymerization conditions.[8]

A variety of crosslinking strategies have been used to create PEG hydrogels that are suitable for both 2D and 3D fibroblast culture applications.[14] These include *i)* PEG-*bis*-acrylate/methacrylate for hydrogel formation by chain growth polymerization and *ii)* multi-arm PEG functionalized with thiols and a variety of alkenes, such as vinyl sulfones, norbornenes, and maleimides, for step growth polymerization.[14] Step-growth chemistries are of particular interest for the rapid formation of hydrogels with MMP-cleavable peptide crosslinks to allow cells to remodel the resulting 3D culture environment.[15–17] In these systems, integrin-binding peptides often have been included to promote specific cell-matrix interactions,

including fibronectin/vitronectin-derived RGDS (binds $\alpha_V\beta_3$ and $\alpha_5\beta_1$ amongst several other integrins),[1,18,19] collagen-derived $(POG)_3POGFOGER(POG)_4$ ($\alpha_1\beta_1$, $\alpha_2\beta_1$)[20,21] and DGEA ($\alpha_2\beta_1$, $\alpha_3\beta_1$),[19,22,23] and laminin-derived IKVAV (laminin receptor).[19,24] Fibroblasts have been shown to respond to variations in receptor-binding peptide composition within these materials. For example, valvular interstitial cells (a type of cardiac fibroblast) were observed to activate in response to the VGVAPG peptide derived from elastin.[25] These systems are also increasingly being used to better understand the role of cell culture geometry in guiding fibroblast activation, for example by comparing fibroblast activation in 2D and 3D cell culture.[26] These PEG-peptide hydrogel systems allow the decoupling of matrix modulus and biochemical content in 2D and 3D culture, with complementarity to the protein-presenting poly(acrylamide) substrates for 2D culture.

These methods of promoting integrin binding used in these common hydrogel culture systems for studying fibroblast activation are both useful for deconstructing the effects of key extracellular cues in cell responses yet have some notable differences. For example, whole proteins present a variety of integrin binding sites and have secondary structure, whereas their peptide mimics generally present one integrin binding sequence and often lack higher ordered structures. Such differences may influence the phenotypes of cells cultured on these biomaterials; however these two methods for promoting integrin binding often are not directly compared in the same culture system, partly owing to differences in materials design and conjugation chemistries. A direct comparison of these two methods for promoting integrin binding could inform comparisons of studies conducted in different material systems and provide insights into the role of integrin binding motifs in promoting fibroblast activation, with relevance for ultimate translation of new material designs and therapeutic strategies in wound healing and fibrosis.

To address this, in this work, we aimed to compare fibroblast activation on two commonly utilized proteins and their peptide mimics: *i)* fibronectin and $PHSRN(G)_{10}RGDS$ (PHSRN-RGDS), where appropriate spacing between RGDS and the PHSRN synergy sequence has been shown to promote binding to $\alpha_5\beta_1$ to mimic aspects of fibronectin,[27] and *ii)* collagen I and $(POG)_3POGFOGER(POG)_4$ (GFOGER), where the triple helical structure imparted by $(POG)_n$ has been shown to promote binding to $\alpha_1\beta_1$ and $\alpha_2\beta_1$ to mimic aspects of collagen I.[28] To enable this comparison, we first established an approach for modifying the surface of step-growth hydrogels with whole proteins. Specifically, we adapted methods using Sulfo-SANPAH chemistry commonly employed to functionalize polyacrylamide hydrogels to modify the surface of step-growth PEG hydrogels that presented amine-functionalized pendant peptides. Both amine-functionalized pendant peptides and integrin binding peptides were incorporated into the hydrogel network using photoinitiated thiol-norbornene click chemistry. With this well-defined system, we examined the phenotype of human pulmonary fibroblasts on these different synthetic matrices, identifying any differences in cell attachment, morphology, and activation, including examination of αSMA expression[29] and YAP nuclear localization, which recently has been shown to be a key step in fibroblast activation.[11] With this approach, we observed important differences in fibroblast response to different substrate compositions, including increased activation on peptide-presenting materials in comparison to their protein counterparts and the formation of activated cell clusters on GFOGER-presenting materials. These studies provide insights into the effects of

integrin binding on fibroblast phenotype, informing the design of materials for modulating fibroblast function and fate *in vitro* and *in vivo*, and a new approach for the presentation of whole proteins from step-growth hydrogel culture systems.

2. Methods

PEG-norbornene functionalization:

Functionalization of multi-arm PEG with norbornenes was performed using an established protocol.[30] Briefly, N,N'-Diisopropylcarbodiimide (DIC) (Sigma) was added to a round bottom flask (5X molar excess relative to the amine functional groups of 8-arm PEG amine). The flask was purged with argon, and then dichloromethane (DCM) was added by syringe while stirring to dissolve the DIC (roughly 30 mL DCM to 2 g DIC). Norbornene carboxylic acid (10X molar excess) (Sigma) was melted anhydrously and transferred by syringe to the flask containing DIC. 8-arm PEG amine (M_n ~ 40 kDa, JenKem) and 4-(dimethylamino)pyridine (DMAP, 0.5X molar excess) (Alfa Aesar) were added to a separate round bottom flask that was then purged with argon, and anhydrous DCM was added to dissolve the PEG and DMAP (roughly 40 mL DCM to 10 g PEG). This polymer solution was transferred to the flask containing the DIC and norbornene solution, which was purged with argon and stirred overnight. The functionalized PEG was purified by precipitation in ice-cold ethyl ether (10X volume) three times with centrifuging between precipitations, dried at room temperature overnight, resuspended in deionized (DI) water, and purified by dialysis against DI water at room temperature for approximately 2 days. The purified polymer was lyophilized and functionality was determined using ^{1}H NMR in D_2O on an AV400 NMR spectrometer: 400 mHz δ 6.15 to 6.0 (m, 16H), δ 3.7 to 3.42 (m, 3636H) and disappearance of the peak at δ 3.12 to 3.02 (t, 16H) (Figure S1). Typical reactions resulted in, on average, ~ 85% norbornene functionality per 8-arm PEG.

Peptide synthesis:

Peptides were synthesized by solid phase peptide synthesis using Fmoc chemistry (Protein Tech Inc PS3, Protein Tech Inc Tribute, or CEM Liberty Blue). All amino acids (APPTec) were double coupled. Sequences G**C**RDVPMS↓MRGGDR**C**G, **C**GGPHSRN$(G)_{10}$RGDS, and **C**GGGK were built on Rink Amide MBHA resin (Novabiochem), and **C**G$(POG)_3$POGFOGER$(POG)_4$G was built on H-Rink Amide-Chemmatrix resin (PCAS Biomatrix). Peptides were cleaved from resin using 95% w/v trifluoroacetic acid (Fisher Scientific), 2.5% w/v triisopropylsilane (Fisher Scientific), and 2.5% w/v DI water. The peptides were cleaved up to 3 hours, precipitated in in ice-cold ethyl ether three times, dried at room temperature overnight, resuspended in DI water, and purified using reverse phase high performance liquid chromatography (HPLC, C18 column, Water:ACN 95:5 to 45:55 over 45 min, Waters). The identity of the peptide sequence was confirmed using electrospray ionization (ESI) mass spectroscopy (Figures S2–S5).

Lithium Phenyl-2,4,6-trimethylbenzoulphosphinate (LAP) synthesis:

The photoinitiator LAP was synthesized by following a previously published protocol.[31] Briefly, dimethyl phenylphosphinate (3 g) (Sigma) and 2,4,6-trimethylbenzoyl (3.2 g) (Sigma) were added to a dry round bottom flask purged with argon and stirred at room

temperature overnight. Lithium bromide (6.1 g) (Sigma) was dissolved in 2-butanone (100 mL) (Sigma) and then added to the round bottom flask. The reaction was heated to 50 °C using an oil bath for 10 minutes. The reaction mixture was cooled over several hours and subsequently filtered to recover the powder product, which subsequently was desiccated under vacuum. The identity of the product was verified by ^{1}H NMR in D_2O: 400 mHz δ 7.59 (m, 2H), 7.44 (m, 1H), 7.36 (m, 2H), 6.78 (s, 2H), 2.12 (s, 3H), and 1.90 (s, 6H).

Hydrogel polymerization:

Hydrogels were formed using thiol-norbornene click chemistry following established protocols.[30] Briefly, a pre-polymerization solution was formed so that the final concentrations of functional groups were 20 mM of norbornene groups from norbornene functionalized 8-arm PEG, 14 mM of thiol groups from the crosslinker G**C**RDVPMS↓MRGGDR**C**G, and 2 mM of thiol groups from the pendant peptide (**C**G(POG)$_3$POGFOGER(POG)$_4$G (GFOGER), **C**GGPHSRN(G)$_{10}$RGDS (PHSRN-RGDS), or **C**GGGK). In the case of GFOGER, the total thiol concentration was decreased to 14 mM by decreasing the amount of thiol contributed by the cross-linker to 12 mM to keep the moduli of the hydrogels consistent among all pendant group compositions. The photoinitiator LAP (2.2 mM) was used in all formulations.

Molds for hydrogel formation were prepared: 10-mm diameter cylinders were punched out of 0.15-mm thick rubber gaskets (McMaster-Carr), and these forms then were pressed onto a Teflon sheet (Protein Technologies, Inc). Glass coverslips (18-mm diameter), for hydrogel immobilization and ease of handling, were thiolated after flame cleaning by incubation in a solution of (3-Mercaptopropyl) trimethoxysilane (170 μL, Sigma) and 190 proof ethanol (30 mL, Fisher) for 5 minutes per side. The coverslips were then rinsed with ethanol and incubated at 80 °C for 15 minutes. The hydrogel precursor solution then was pipetted into the molds and covered with the thiolated coverslip. The solution was exposed to 10 mW/cm^2 at 365 nm for 5 minutes using an Omnicure Series 2000 (Excilitas, Waltham, MA) with a 365 nm filter, light guide, and collimating lens (Exfo; intensity measured with NIST Light Measurement System from International Light). The resulting hydrogels covalently immobilized to glass coverslips were swollen in phosphate buffered saline (PBS) with 1% penicillin/streptomycin (Life Technologies) and 0.2% fungizone (Thermo Fisher) and sterilized by exposure to germicidal UV (Spectroline model EF-180) for 15 minutes. For modulus measurements, hydrogels were polymerized *in situ* with an AR-G2 rheometer with UV light accessory and 8-mm geometry (10 mW/cm^2 at 365 nm) (TA Instruments; Omnicure Series 2000, Exfo). During polymerization, shear modulus was measured over time at a strain of 1% and a frequency of 2 Hz for measurements within the linear viscoelastic regime. The final modulus (e.g., no measurable change in modulus with continued irradiation) was generally reached within two minutes of commencing irradiation. Young's modulus then was calculated using rubber elasticity theory, adjusting for theoretical equilibrium swelling.[32,33]

Protein conjugation:

Whole proteins (rat tail collagen I (BD), fibronectin (Corning), or FITC-labeled collagen) were conjugated to amines presented by hydrogels containing pendant CGGGK using the

heterobifunctional linker Sulfo-SANPAH, adapting protocols previously utilized with polyacrylamide hydrogels.[9] Specifically, CGGGK-presenting hydrogels were swollen in PBS overnight and then immersed in a 1-mg/mL solution of Sulfo-SANPAH in HEPES buffer (pH ~ 8). The hydrogels then were exposed to 10 mW/cm^2 at 365 nm for 15 minutes and washed 3X (20-min each) with fresh HEPES buffer. Modified hydrogels then were covered with either collagen I in HEPES buffer (pH ~ 6) or fibronectin in neutral HEPES buffer and incubated at 4 °C overnight for covalent immobilization of the respective protein. The resulting hydrogel substrates subsequently were washed 3X with sterile PBS. For the encapsulation of fibronectin, protein solution was added to the hydrogel precursor solution at a concentration of 300 nM.

Characterization of peptide incorporation:

Fluorescently-labeled model peptide tether (CGRGDS-Ahx-AF488) was synthesized according to published protocols.[34] Briefly, after removal of the Fmoc on the N'-terminus of the peptide, the resin was transferred from the automated peptide synthesizer to a reaction vessel and stirred overnight with 1 mg of Alexa Fluor 488 Carboxylic Acid, 2,3,5,6-Tetrafluorophenyl Ester, 5-isomer (Invitrogen) in 4 mL of DMF and 50 μL of N,N'-diisopropylethylamine (DIPEA) (Chem-Impex International). The resulting fluorescently-labeled peptide then was cleaved from resin, purified by HPLC, and analyzed by ESI-MS as described above.

To create a standard curve for relating hydrogel fluorescence to peptide concentration, hydrogels (30 μL) with no pendant peptide were polymerized in cylindrical molds (5-mm diameter) then swollen in standard solutions of fluorescent peptide in PBS (0 mM, 0.2 mM, 1 mM, and 2 mM) on a shaker in the dark overnight. The next day the hydrogels were moved to new well plates and imaged on a confocal microscope (LSM 810, Zeiss). Each standard condition was replicated in triplicate.

To measure peptide incorporation, hydrogels were polymerized in cylindrical molds (~5-mm diameter) with 2 mM fluorescently-labeled peptide included in the pre-polymerization solution, as done with other pendant peptides. Hydrogels were polymerized (10 mW/cm^2 at 365 nm for 5 minutes) and swollen in PBS overnight in the dark. The resulting hydrogels with immobilized peptide tethers were imaged at the same time as the hydrogels swollen with different concentrations of fluorescently-labeled peptide for the standard curve. Hydrogels were imaged on an LSM 810 confocal microscope (Zeiss) (n=3). The total fluorescence intensity of each image was measured using ImageJ. Linear regression was used to produce a trend line from the standard curve for calculating the concentration of peptide incorporated into the hydrogel network.

Cell culture:

Human pulmonary fibroblasts (CCL151, ATCC) were cultured in Ham's F12K medium (Life Technologies) with 10% fetal bovine serum (Invitrogen), 1% penicillin/streptomyocin (Life Technologies), and 0.2% fungizone (Thermo Fisher). Cells were propagated on tissue culture plastic, feeding every 2–3 days and passaging at 80% confluency (passage 15 to 18 used in all experiments). Normal Human Lung Fibroblasts (Lonza) were cultured in FGM-2

medium (Lonza). Cells were propagated on tissue culture plastic, feeding every other day and passaged at 80% confluency (passage 6 to 8 in all experiments) according to vendor instructions. Note, while propagation on tissue culture plastic is standard practice, culturing of fibroblasts on such substrates that are 'stiff' relative to native soft tissues is known to promote some level of fibroblast activation during propagation[35,36] that would be present at the start of each experiment.

Immunostaining:

At time points of interest hydrogels were washed with PBS and then fixed with 4% PFA (Fisher Scientific) for 15 minutes at room temperature. Fixed samples were washed with PBS (4X for 5 minutes each) and then blocked with 5% BSA in PBS for one hour while rocking. If necessary (i.e., for cell studies but not protein-only studies), hydrogel samples were permeabilized with 0.2% v/v triton-X (Fisher Scientific) for 15 minutes and then washed in 0.2% (v/v) Tween-20 (Sigma) (4X for 5 minutes each) while rocking. Primary antibody with 1.5% BSA in PBS (rabbit anti-YAP (Abcam ab52771, 1:200), mouse anti-alpha smooth muscle actin (Abcam ab7817, 1:50), rabbit anti-collagen (Abcam ab34710, 1:200), or mouse anti-fibronectin (Abcam ab26245, 1:200) was added to blocked samples and incubated at 4°C overnight. The samples were washed with 0.2% (v/v) Tween-20 (4X for 5 minutes each) while rocking. The secondary antibody (1:200) (goat anti-rabbit AlexaFluor 594 (Invitrogen A11012), goat anti-mouse AlexaFluor 488 (Invitrogen A1101), or goat anti-rabbit AlexaFluor 647 (Invitrogen A21244)) and rhodamine-labeled phalloidin to label F-actin (5 μg/mL) (Sigma) were added in a 1.5% BSA in PBS solution and incubated overnight at 4 °C. Hydrogels were washed with PBS (4X for 5 minutes each) while rocking and incubated with DAPI (Invitrogen) for 5 min. Hydrogels were stored in PBS at 4 °C protected from light until imaging.

For counting live cells at 24 hours in culture to assess initial cell attachment, samples without any fixation were stained with Hoescht dye only. Specifically, Hoescht 33258 was diluted in PBS to a concentration of 5 μg/mL and incubated with live samples at 37 °C for 30 minutes. The Hoescht solution was replaced with warmed PBS, and three hydrogels were imaged for every condition and three images were taken per hydrogel. Error was calculated using n=3 hydrogels.

Imaging:

Samples were imaged on either an LSM 810 or LSM META 510 Confocal Microscope (Zeiss). Images were taken as 100-micron z-stacks with imaging parameters kept consistent between different conditions. Samples with proteins conjugated to the surface of Sulfo-SANPAH functionalized hydrogels were imaged on an Axio Observer A1 Inverted Epi-fluorescence Microscope (Zeiss). In all cases, three images or more were taken per replicate (>100 cells counted per condition), and care was taken to avoid imaging near the edges of the hydrogels.

Image analysis for cell number and αSMA expression using Fiji:

Confocal z-stacks were converted to maximum intensity projections in Fiji, and then the channels were split. The nuclei were counted to assess cell number. The 405-nm (DAPI)

channel subsequently was merged with the 488-nm (αSMA) channel, and the number of nuclei associated with αSMA was determined to quantify the percentage of cells positive for αSMA. Error was calculated using n=9 hydrogels for CCL151 studies and n=3 hydrogels for NHLF studies.

$$\% \ positive = \ \# \ of \ cells \ positive \ for \ \alpha SMA / total \ nuclei$$

Image analysis for YAP nuclear localization in Volocity:

YAP nuclear localization was assessed following a modified version of published protocols.[11,37] Briefly, the "Find Objects" function in Volocity (PerkinElmer) was used to find nuclei and cell bodies (f-actin) in the DAPI (405 nm) and red (594 nm) channels, respectively. The "Analyze" function then was used to determine the mean fluorescence intensity for YAP in the far red channel (647 nm). Fluorescence intensity localized to the nucleus vs. the cytosol (i.e., nuclear YAP vs. cytosolic YAP) was quantified by identifying nuclei as "Population 1," cell bodies as "Population 2", and subtracting the mean fluorescence for Population 1 from Population 2 using the "Subtract" function.

Statistical analysis:

Results are reported as mean ± standard error with n ≥ 3 for all conditions, where exact numbers of replicates are noted above for specific experiments. To determine statistical significance ($p < 0.05$), a two-tailed t-test was performed using Excel.

3. Results and Discussion

3.1. Approach for incorporation of whole proteins or synthetic integrin-binding peptides into a step growth hydrogel culture platform

We formed hydrogels using photoinitiated, step growth thiol-ene click chemistry to allow incorporation of pendant peptides during hydrogel formation and control of matrix modulus, with relevance for both 2D and 3D cell culture.[20,26] Eight-arm PEG functionalized with norbornene end groups (PEG-8-**NB**, M_n ~ 40,000 g/mol) was reacted with an MMP-degradable synthetic peptide presenting pendant thiols (G**C**RDVPMS↓MRGGDR**C**G) in the presence of a photoinitiator LAP and light (10 mW/cm^2 at 365 nm for 5 min) (Figure 1) (reactive functionality **bolded**). This thiol-norbornene reaction scheme produced hydrogels with tunable mechanical properties (Young's modulus (E) ~ 5 to 25 kPa) relevant for mimicking soft tissues (e.g., healthy to fibrotic connective tissues such as lung) (Figure 1), and while not utilized in this work, enables the encapsulation of cells during gel formation for 3D culture applications.[12,33,38–40] We chose to focus our study on fibroblast activation in 2D culture, as most studies conducted in the polyacrylamide-protein system are in two dimensions, and using a matrix modulus known to promote fibroblast activation (E ~ 15 kPa) toward elucidating any differences in activation in response to the selected ECM proteins and their peptide mimics.[5,41]

Peptides were reacted into the hydrogel during network formation by photoinitiated thiol-ene click chemistry. Specifically, a cysteine was incorporated into peptide sequences of

interest to conjugate them into the network as pendant peptides: *i)* GFOGER sequence **C**G(POG)$_3$POGFOGER(POG)$_4$G and *ii)* PHSRN-RGDS sequence **C**GGPHSRN(G)$_{10}$RGDS for integrin binding or *iii)* **C**GGG**K** for subsequent conjugation with whole proteins as described below. Interestingly, because the GFOGER peptide self assembles to form triple helices,[20,21] its inclusion in the pre-polymerization solution was observed to produce a slight increase the modulus of the final hydrogel; this effect was counteracted by a slight decrease in the amount of crosslinking peptide within hydrogels containing GFOGER (Figure S6). With this approach, hydrogels were synthesized with a consistent modulus of E ~ 15 kPa for all pendant peptide compositions.

We prepared substrates with 2 mM pendant peptide in the hydrogel precursor solution as this concentration during hydrogel preparation previously had been shown to promote cell adhesion and response with PEG-based thiol-norbornene hydrogels in both 2D and 3D culture.[23,25,26,33] To determine the amount of pendant peptide presented by these materials after hydrogel formation and swelling, we examined the concentration of a fluorescently-labeled model pendant peptide (**C**GRGDS-AF488) incorporated within each hydrogel. Fluorescence of the resulting hydrogel was compared to that of hydrogels swollen in known concentrations of fluorescently-labeled peptide: samples were imaged with a confocal microscope to generate a calibration curve from which the concentration of conjugated fluorescently-labeled peptide was calculated, following an approach previously reported by others.[23] Using this technique we determined that the concentration of the peptide immobilized within the hydrogels was approximately 0.25 mM, which is consistent with literature reports for other photopolymerized thiol-norbornene hydrogels.[23]

While many methods exist for incorporating large structural ECM proteins into synthetic hydrogels, including encapsulation during hydrogel formation or surface conjugation via a covalent linker, we aimed to use Sulfo-SANPAH conjugation for the functionalization of hydrogels in this work, with complementarity to the widely used in polyacrlamide-based *in vitro* model systems.[9,13,42–44] Sulfo-SANPAH contains two amine reactive functional groups, an activated ester and a light-sensitive azide, making it well suited as a heterobifunctional linker for covalent immobilization of amine-containing proteins to amine-presenting substrates like polyacrylamide. However, hydrogels formed by thiol-ene step growth polymerization do not inherently present such free amines. Here, we sought to establish a new approach for immobilization of proteins on the surface of these hydrogels built upon the success of using Sulfo-SANPAH for modification of polyacrylamide hydrogels used for 2D culture.

Amine-bearing peptide tethers were incorporated during hydrogel formation by reacting in a pendant **C**GGG**K** sequence. Free amines on the hydrogel surface then were reacted with Sulfo-SANPAH in the presence of UV light (365 nm at 10 mW/cm^2 for 15 minutes), making the hydrogel surface reactive to amine containing proteins, such as collagen I and fibronectin, through the immobilization of the linker presenting an activated ester. Hydrogels and protein solution (50 μg/mL collagen I or 132 μg/mL fibronectin, similar concentrations to those previously used in the literature, as detailed below)[5,43] were incubated at 4 °C overnight in the dark for reaction with the activated ester linker. We confirmed consumption of amines presented from the peptide tethers and respective ECM proteins upon reaction

with the Sulfo-SANPAH linker using a fluorescence-based assay for assessing total amine content (fluoraldehyde-OPA) (Figure 2). Additionally, we observed presentation of whole proteins (fibronectin or collagen I) from the surface of the hydrogels after conjugation using immunostaining and epifluorescence microscopy (Figure 2) and did not observe significant protein loss in wash solutions (Figure S7), suggesting good retention upon immobilization. Taken together, these data support covalent immobilization of each ECM protein on the hydrogel surface. This approach provides a step-growth hydrogel analog to polyacrylamide systems modified with whole proteins for 2D culture applications.

3.2 Protein and peptide concentrations identified for consistent attachment of cells between compositions

A variety of fibronectin and collagen concentrations have been used in various *in vitro* cell culture models models.[5,35,41,45–47] To choose appropriate protein concentrations for comparison of whole proteins and their peptide mimics, we considered protein concentrations that had previously been utilized as well as the effect protein concentration would have on cell density. As a starting point for comparisons, protein concentrations for collagen I or fibronectin, respectively, first were selected based on those typically used in the literature for similar hydrogel-based culture substrates that have been used for fibroblast culture and cell attachment (50 μg/mL collagen I or 132 μg/mL (300 nM) fibronectin).[5,43] However, cell-cell contact also is a key consideration, particularly in studies of fibroblast activation: during fibrosis, cell-cell contact and the formation of adherens junctions increases and have been shown to influence fibroblast activation.[48] Consequently, to limit the confounding effects of different levels of cell-cell contact, at least initially, protein concentrations that promoted similar levels of initial cell attachment as their peptide counterparts where identified. Specifically, cell attachment to protein-functionalized substrates at 24 hours was compared to cell attachment to their respective peptide mimics (GFOGER or PHSRN-RGDS, 2 mM in hydrogel formulation, respectively), and protein concentrations were adjusted for achieving similar seeding densities. Here, human pulmonary fibroblasts were selected as a model fibroblast cell type.

For collagen- and GFOGER-functionalized substrates, we observed higher levels of cell adhesion to hydrogels functionalized with collagen I at concentrations previously reported in the literature, starting with 50 μg/mL,[5] as compared to hydrogels functionalized with GFOGER peptide (24 hours in cell culture) (Figure 3). Lower concentrations of collagen (0.5 to 5 μg/mL) subsequently were investigated, where a concentration of 5 μg/mL collagen I was observed to yield the same initial cell density as the GFOGER peptide. Consequently, to keep cell-cell contact initially constant between these protein- and peptide-functionalized substates, we used the 5 μg/mL collagen I for subsequent comparisons of fibroblast phenotype on collagen- and GFOGER-functionalized hydrogels.

Similarly, fibronectin was conjugated to hydrogel surfaces as detailed above. At 24 hours, cell density was compared between fibronectin- and PHSRN-functionalized substrates. Fewer fibroblasts were present on the fibronectin-functionalized hydrogel surface at this early timepoint (Figure S8). As the concentration of fibronectin used was already at a high level in the context of the literature, we hypothesized that the Sulfo-SANPAH conjugation,

which non-specifically reacts with free amines presented by proteins, may have affected the structure or presentation of key binding sites on fibronectin or obscured parts of the protein that promote cell adhesion. To partly test this and ultimately circumvent this issue, fibronectin at the same concentration (132 μg/mL (300 nM)) was encapsulated, as opposed to covalently conjugated, within the hydrogel during hydrogel formation, an approach that had been previously utilized for PEG-based hydrogels in the 2D culture of valvular fibroblasts.[43] During sample washes, we observed loss of approximately 15% of the encapsulated protein, likely due to minor burst release or removal of loosely adsorbed protein upon equilibrium swelling of the hydrogels after formation, suggesting that 85% of fibronectin from the precursor solution was entrapped and retained in the hydrogel for cell culture (Figure S7). When comparing initial cell seeding between samples with entrapped vs. covalently-conjugated protein, we observed that cell attachment increased on hydrogels containing encapsulated fibronectin in comparison to those with Sulfo-SANPAH-conjugated fibronectin, despite the fact that the Sulfo-SANPAH condition presumably presented a higher concentration of fibronectin on the surface of the sample. This result further suggests that the process of covalently conjugating fibronectin to the hydrogel surface with Sulfo-SANPAH impacted fibroblast-fibronectin interactions. Initial cell seeding densities on hydrogels containing encapsulated fibronectin were similar to those on PHSRN-RGDS-functionalized hydrogels (Figure S9). Consequently, to proceed with comparison of fibroblast phenotype on fibronectin- and PHSRN-RGDS-functionalized hydrogels, encapsulated fibronectin was used for all substates in subsequent cell culture experiments.

3.3 Comparison of fibroblast morphology and phenotype on hydrogels functionalized with whole proteins or integrin binding peptides

Fibroblasts are known to respond to changes in the ECM during would healing by expressing αSMA to enable contraction and secreting and new ECM proteins, including large amounts of collagen I, to remodel and repair the injured tissue.[1–3] Further, the YAP/TAZ signaling pathway, which is involved in a number of cellular processes including mechanotransduction, recently has been identified as a driver of fibroblast activation, where increased YAP nuclear localization correlates with increased activation and has been observed in fibrotic lung tissue.[11,37,41] To assess fibroblast response to our different protein- and peptide-functionalized substrates, we thus examined cell morphology (staining for cytoskeletal protein F-actin) and αSMA and YAP expression as hallmarks of fibroblast activation (Figure 4). Human pulmonary fibroblasts were seeded on hydrogels presenting fibronectin, PHSRN-RGDS, collagen I, or GFOGER, respectively. At 72 hours, samples were fixed and stained to assess activation, where sufficient time was given to observe a robust cell response to the underlying matrix at both the cellular and protein levels.[43,49] Cell morphology was slightly rounded on hydrogels functionalized with fibronectin and PHSRN-RGDS, whereas fibroblasts adopted a spread and elongated morphology on collagen I-functionalized hydrogels and formed star-shaped clusters on GFOGER-functionalized hydrogels. Additionally, while all complementary protein and peptide samples started at the same initial cell density (as shown in Figure 3), cell number was roughly three times higher on the collagen-functionalized hydrogels compared to the other conditions by 72 hours.

Both fibronectin and PHSRN-RGDS promoted high levels of αSMA expression. However, statistically more fibroblasts were αSMA positive on PHSRN-RGDS-functionalized hydrogels (86 ± 1.9%) than on fibronectin-functionalized hydrogels (70 ± 2.6%) ($p < 0.01$). YAP nuclear localization was not statistically different between the two conditions. These results suggest that, while cells did not appear to spread on these motifs, fibroblasts adhered and responded to either whole fibronectin or the PHSRN-RGDS peptide mimic, expressing early markers of myofibroblastic activation like αSMA expression throughout the cell body. Additionally, while the majority of fibroblasts in both conditions were activated, these observations suggest that the peptide sequence promoted slightly more activation than the whole protein at the concentrations probed, potentially owing to its increased targeting of specific integrins (namely, $\alpha_5\beta_1$). These findings correlate to previously published observations of fibroblasts expressing high levels of αSMA on stiff RGD-containing hydrogels,[50] and the essential role of fibronectin in the development of fibrosis.[51,52]

Fibroblasts were observed to exhibit both different morphologies and levels activation on GFOGER-functionalized hydrogels and collagen I-functionalized hydrogels (Figure 4), as well as different cell numbers by 72 hours while having starting at similar initial cell densities (Figure 3). Significantly fewer fibroblasts expressed significant levels of αSMA (18 ± 4.6%) on collagen-functionalized hydrogels, despite increased cell-cell contact which one might expect to be activating,[48] as compared to GFOGER-functionalized hydrogels αSMA (89 ± 2%) ($p < 0.01$). A statistically significant decrease in YAP nuclear localization also was observed on collagen I-functionalized hydrogels relative to GFOGER ($p < 0.05$).

These results suggest that, under the conditions probed, fibroblasts activate significantly more in response to the collagen-mimicking GFOGER peptide than its whole protein counterpart collagen I. In addition to the observed expression of markers of activation, the star shaped clusters observed on the GFOGER peptide are reminiscent of fibroblast foci that are observed in fibrotic disease.[53] To ensure that this interesting response was not cell line specific, we replicated this experiment with primary normal human lung fibroblasts (Lonza) and observed similar responses as observed with the banked human pulmonary fibroblasts (CCL-151) (Figure S10).

The differences observed between GFOGER and collagen I, and to a lesser extent between PHSRN-RGDS and fibronectin, are useful both for comparing results among models that use these proteins or peptides to influence cell behavior and for understanding fibroblast activation in fibrosis. In healthy human lung tissue, fibronectin is present but at lower levels than laminin or collagen I in the lung epithelium or interstitium, respectively, and often associated with proteins in the basement membrane or with collagen fibrils.[54] After injury, increasing amounts of fibronectin are produced and accumulate in the provisional matrix during tissue remodeling. The high levels of fibroblast activation observed in both the fibronectin and PHSRN-RGDS conditions may be reminiscent of cell response during this process, where a stiff synthetic matrix rich in fibronectin or PHSRN-RGDS may mimic aspects of fibronectin accumulation during the progression of lung fibrosis. Indeed, fibronectin has been observed to be associated with activated fibroblast foci, suggesting that the protein may contribute to fibroblast activation or persistence.[54] Alternatively, collagens, particularly type IV in the epithelium and type I in the interstitium, are ubiquitous

throughout the lung, making up 15% of the dry weight of a healthy human lung. During fibrosis, collagen degradation decreases while collagen synthesis and crosslinking increases, leading to the accumulation of a stiff and disordered collagen-rich matrix.[54] The GFOGER condition, perhaps by increased targeting of β1, may mimic aspects of this disordered, high-collagen environment that contributes to fibroblast activation and persistence. To better understand the differences observed between the collagen and GFOGER conditions, we conducted a series of experiments to further characterize fibroblast phenotype on these materials.

3.4 Probing differences in cell response to GFOGER- and collagen-functionalized hydrogels

To better understand the origin of the clustering behavior observed on GFOGER hydrogels, we monitored human pulmonary fibroblasts cultured on GFOGER-functionalized hydrogels over time (at 6, 12, 24, and 72 hours). Fibroblasts initially seeded as individual cells on the hydrogels and formed clusters over time (Figure 5). Image analysis revealed that the number of objects in the images decreased over time while cell number remained relatively consistent (number of nuclei from DAPI staining), suggesting the formation of clusters by migration of cells initially seeded onto the substrate rather than the proliferation of cells on the substrate. The resulting clusters are reminiscent of foci in fibrotic tissue.[53]

These observations of clustering along with the high levels of αSMA observed for cells on GFOGER-functionalized matrices may suggest that targeting and increased binding of specific integrins by the integrin-binding peptide (e.g., $\alpha_2\beta_1$ and $\alpha_1\beta_1$) relative to the whole protein induced more disease-like behavior in pulmonary fibroblasts. Broadly, while peptides often target a few specific integrins, whole proteins present several different integrin-binding sequences. Additionally, large portions of proteins are not integrin targeting yet may affect cell behavior by sequestering cytokines. In particular, the GFOGER peptide is known to target integrins $\alpha_2\beta_1$ and $\alpha_1\beta_1$, whereas collagen I contains sequences known to bind $\alpha_2\beta_1$, $\alpha_1\beta_1$, $\alpha_3\beta_1$, $\alpha_V\beta_3$, as well as many other integrins.[55] To understand more specifically the representation of GFOGER-like sequences within whole collagen for comparison, we performed a search of such integrin-binding subunits within collagen I.

Specifically, collagen is a polymeric protein made up of alpha 1 and alpha 2 chains, and the typical collagen I monomer contains two alpha 1 chains and one alpha 2 chain (total molecular weight of 407 kDa (National Center for Biotechnology Information)). Only the alpha 1 chain contains the GFOGER sequence (1 per strand; National Center for Biotechnology Information). Using this information we estimated that hydrogels modified with 5 μg/mL collagen I contain up to 24.5 nM of the GFOGER sequence. Both the alpha 1 and alpha 2 chains of collagen I contain 9 GFOGER-like GER sequences (GXXGER: GROGER, GLOGER, GPOGER, GKAGER, GARGER, GGRGER, GASGER, GPAGER), resulting in 18 GFOGER-like GER sequences per collagen monomer. With this, we calculated that collagen-functionalized hydrogels contain up to 0.22 μM GFOGER-like sequences. Taken together, collagen-functionalized hydrogels were estimated to contain significantly fewer $\alpha_2\beta_1$ and $\alpha_1\beta_1$ integrin targeting sequences relative to GFOGER-functionalized hydrogels, which contain approximately 0.25 mM of pendant peptide that

targets $\alpha_2\beta_1$ and $\alpha_1\beta_1$. For comparison, we conducted a similar calculation to examine any differences in $\alpha_5\beta_1$-binding sites between the fibronectin and PHSRN-RGDS conditions. We estimated that 85% of encapsulated fibronectin was retained in the hydrogel (Figure S7), leading to a concentration of approximately 0.25 μM of entrapped fibronectin within the hydrogels for fibroblast culture. With one PHSRN-RGDS sequence per fibronectin, the amount of PHSRN-RGDS presented by the fibronectin-presenting hydrogels would be roughly three orders of magnitude less than the approximately 0.25 mM of PHSRN-RGDS sequence presented by the PHSRN-RGDS-functionalized hydrogels.

Collagen deposition is a hallmark of pulmonary fibrosis. Given this physiological context and our estimated mismatch in GXXGER integrin-binding sequences between peptide versus protein-functionalized samples we hypothesized that increasing the amount of collagen I functionalized to the hydrogel, which would increase the number of integrin-binding sites presented by the whole protein samples, would increase the percentage of activated fibroblasts. To investigate this, we conjugated higher concentrations of collagen I to the surface of hydrogels (over two orders of magnitude: 5, 50, and 500 μg/mL) and compared percentage of αSMA expressing fibroblasts. These condiditions included the 5 μg/mL concentration of collagen I initially tested and GFOGER-functionalized hydrogels for comparison. Collagen I labeled with AlexaFluor-488 was used during sample preparation to allow visual confirmation of collagen presentation. The surface of hydrogels that had been functionalized with Sulfo-SANPAH and incubated with solutions of different concentrations of fluorescently-labeled collagen I, ranging from 5 to 500 μg/mL, subsequently was imaged using confocal microscopy and relative fluorescence intensity quantified. Increased fluorescence was observed with increasing collagen I concentration, indicating that increased concentrations in collagen I applied to the Sulfo-SANPAH-functionalized hydrogels resulted in increased collagen I presented on the surface (Figure 6A).

Using this approach, hydrogels were functionalized with different concentrations of standard, unlabeled collagen I and used to culture fibroblasts (Figure 6B–D). As before, samples were fixed and stained at 72 hours in culture to assess cell response (F-actin, αSMA, and DAPI nuclear stain). A trend of increasing αSMA positive cells was observed with increasing collagen I concentration; however, the differences between conditions were not statistically signficant. An elongated cell morphology was observed on all collagen functionalized substrates, with some clusters of cells present on the highest concentration of collagen I. Cell clustering and the percentage of αSMA cells still were significantly increased for GFOGER-functionalized substrates in comparison with all collagen I conditions tested. Note, while samples functionalized with 5 μg/mL collagen I and GFOGER, respectively, began with a similar cell seeding density, increased number of cells were observed on all collagen I-functionalized substrates relative to the GFOGER-functionalized substrate by 72 hours. Decreased proliferation often is commensurate with increased activation of fibroblasts: for example, in the early stages of wound healing, fibroblasts migrate to the site of injury and proliferate, and as they transition to more mature myofibroblasts, proliferation decreases and matrix remodeling increases.[37] This transition that occurs with increased activation could explain the difference in cell number at 72 hours between all collagen- and GFOGER-functionalized hydrogels.

These studies suggest that the differences observed in fibroblast phenotype between collagen I- and GFOGER-functionalized hydrogels may be the result of several differences between the protein and peptide conditions and not be strictly a concentration effect. Indeed, significantly lowering the GFOGER concentration (0.1 mM vs. 2 mM GFOGER at hydrogel formation) did not result in statistically significant decrease in the percentage of αSMA positive cells (Figure S11). Many differences between the collagen-functionalized hydrogels and GFOGER-functionalized hydrogels, including but also beyond concentration, could be contributing to these results as a whole. For example, in addition to the differences between the concentration of integrin binding sites, the structure of collagen I (e.g., fibrils) on the surface of these hydrogels likely differs from the structure of the GFOGER sequence. Further, collagens also sequester growth factors and may serve as local reservoirs for soluble factors found within serum-containing media or target other integrins. The challenge of decoupling these many, possibly interacting, factors underscores the need for a better understanding of the many ways cells and different proteins interact in fibrosis. Well-defined hydrogel systems that allow us to mimic aspects of whole proteins with combinations of peptides and polymers (e.g., matrix integrin-binding, mechanical properties) for hypothesis testing may be useful tools for conducting these studies. For such future studies, the activating-nature of the GFOGER sequence may prove useful for probing aspects of fibroblast activation and persistence in fibrotic disease, or more broadly, as a handle for modulating activation in the context of other extracellular cues (e.g., matrix integrin-binding, modulus, structure). By intentionally choosing a controlled integrin binding technique, as done here, or by controlling the biophysical properties of the matrix, the complexity of the ECM can be deconstructed toward elucidating the role of these extracellular cues in directing cell functions and fate with relevance for the design of therapeutic interventions.

3. Conclusions

In this work, we introduced a method for conjugating whole proteins to hydrogels that had been polymerized by a step growth thiol-ene reaction for controlled cell culture applications. We used this technique to compare the activation of human pulmonary fibroblasts on whole proteins important in wound healing (collagen I and fibronectin) and their peptide mimics (GFOGER and PHSRN-RGDS). We found that fibronectin and PHSRN-RGDS induced similar cell morphologies, and PHSRN-RGDS promoted a slight yet statistically significant increase in the percentage of cells expressing αSMA. Interestingly, we found that collagen I induced a more elongated fibroblast morphology and fewer fibroblasts expressing αSMA than GFOGER. On GFOGER, activated clusters of fibroblasts were observed to form over time, reminiscent of fibroblast foci and suggesting the potential a role for $\alpha_2\beta_1$ and $\alpha_1\beta_1$ in the progression of fibrosis for future investigations. These findings highlight the need for well-defined hydrogel systems for examining the effects of integrin binding on cell behavior, where the complexity of matrix structure, mechanical properties, and biochemical content can be decoupled. By understanding how the concentration, identity, and presentation of integrin binding sites contained in a synthetic matrix affect fibroblast activation, it is possible to better design materials that mimic aspects of *in vivo* conditions toward understanding and directing wound healing and fibrotic disease.

Supplementary Material

Refer to Web version on PubMed Central for supplementary material.

Acknowledgements

This work was supported by a National Science Foundation Career Award (DMR-1253906), the Pew Charitable Trusts (00026178), and the Delaware COBRE programs in Drug Discovery and in Advanced Biomaterials funded by Institutional Development Awards from the National Institute of Generals Medical Sciences at the National Institutes of Health (P20GM104316 and P30GM110758, respectively). Additionally, the authors thank Prof. Wilfred Chen and Prof. Millicent Sullivan for access to specific instruments and reagents and the DBI Bioimaging center.

References

(1). Kyburz KA; Anseth KS Synthetic Mimics of the Extracellular Matrix: How Simple Is Complex Enough? Ann. Biomed. Eng 2015, 43 (3), 489–500. 10.1007/s10439-015-1297-4 [PubMed: 25753017]

(2). Hansen NUB; Genovese F; Leeming DJ; Karsdal MA The Importance of Extracellular Matrix for Cell Function and in Vivo Likeness. Exp. Mol. Pathol 2015, 98 (2), 286–294. 10.1016/j.yexmp.2015.01.006 [PubMed: 25595916]

(3). Klingberg F; Hinz B; White ES The Myofibroblast Matrix: Implications for Tissue Repair and Fibrosis. J. Pathol 2013, 229 (2), 298–309. 10.1002/path.4104 [PubMed: 22996908]

(4). Sethi KK; Yannas IV; Mudera V; Eastwood M; McFarland C; Brown R A. Evidence for Sequential Utilization of Fibronectin, Vitronectin, and Collagen during Fibroblast-Mediated Collagen Contraction. Wound Repair Regen 2002, 10 (6), 397–408. 10.1046/j.1524-475X.2002.10609 [PubMed: 12453144]

(5). Liu F; Mih JD; Shea BS; Kho AT; Sharif AS; Tager AM; Tschumperlin DJ Feedback Amplification of Fibrosis through Matrix Stiffening and COX-2 Suppression. J. Cell Biol 2010, 190 (4), 693–706. 10.1083/jcb.201004082 [PubMed: 20733059]

(6). Goffin JM; Pittet P; Csucs G; Lussi JW; Meister J-J; Hinz B Focal Adhesion Size Controls Tension-Dependent Recruitment of Alpha-Smooth Muscle Actin to Stress Fibers. J. Cell Biol 2006, 172 (2), 259–268. 10.1083/jcb.200506179 [PubMed: 16401722]

(7). Smithmyer ME; Sawicki LA; Kloxin AM Hydrogel Scaffolds as in Vitro Models to Study Fibroblast Activation in Wound Healing and Disease. Biomater. Sci 2014, 2 (5), 634–650. 10.1039/C3BM60319A [PubMed: 25379176]

(8). Kandow CE; Georges PC; Janmey P A; Beningo, K. A. Polyacrylamide Hydrogels for Cell Mechanics: Steps toward Optimization and Alternative Uses. Methods Cell Biol 2007, 83 (7), 29–46. 10.1039/C3BM60319A [PubMed: 17613303]

(9). Wang Yu-Li, Pelham RJ Cell Locomotion and Focal Adhesions Are Regulated by Substrate Flexibility. Proc. Am. Thorac. Soc 1997, 94, 13661–13665. 10.1073/pnas.94.25.13661

(10). Denisin AK; Pruitt BL Tuning the Range of Polyacrylamide Gel Stiffness for Mechanobiology Applications. ACS Appl. Mater. Interfaces 2016, 8 (34), 21893–21902. 10.1021/acsami.5b09344 [PubMed: 26816386]

(11). Liu F; Lagares D; Choi KM; Stopfer L; Marinković A; Vrbanac V; Probst CK; Hiemer SE; Sisson TH; Horowitz JC; et al. Mechanosignaling through YAP and TAZ Drive Fibroblast Activation and Fibrosis. Am. J. Physiol. Lung Cell. Mol. Physiol 2014, 5308, L344–L357. 10.1152/ajplung.00300.2014

(12). Engler AJ; Sen S; Sweeney HL; Discher DE Matrix Elasticity Directs Stem Cell Lineage Specification. Cell 2006, 126 (4), 677–689. 10.1016/j.cell.2006.06.044 [PubMed: 16923388]

(13). Stephanie A. Fisher Alexander E.G. Baker; Shoichet MS Designing Peptide and Protein Modified Hydrogels: Selecting the Optimal Conjugation Strategy. Neurologic Clinics 2017, pp 7416–7427. 10.1021/jacs.7b00513

(14). Kharkar PM; Kiick KL; Kloxin AM Designing Degradable Hydrogels for Orthogonal Control of Cell Microenvironments. Chem. Soc. Rev 2013, 42 (17), 7335–7372. 10.1039/c3cs60040h [PubMed: 23609001]

(15). Lutolf MP; Lauer-Fields JL; Schmoekel HG; Metters AT; Weber FE; Fields GB; Hubbell JA Synthetic Matrix Metalloproteinase-Sensitive Hydrogels for the Conduction of Tissue Regeneration: Engineering Cell-Invasion Characteristics. Proc. Natl. Acad. Sci. U. S. A 2003, 100 (9), 5413–5418. 10.1073/pnas.0737381100 [PubMed: 12686696]

(16). Patterson J; Hubbell JA Enhanced Proteolytic Degradation of Molecularly Engineered PEG Hydrogels in Response to MMP-1 and MMP-2. Biomaterials 2010, 31 (30), 7836–7845. 10.1016/j.biomaterials.2010.06.061 [PubMed: 20667588]

(17). Hahn Mariah S, Liao Huimin, Munoz-Pinto Dany, Qu Xin, Hou Yaping, Grunlan MA Influence of Hydrogel Mechanical Properties and Mesh Size on Vocal Fold Fibroblast Extracellular Matrix Production and Phenotype. Acta Biomater 2012, 76 (10 2009), 211–220. 10.1016/j.actbio.2008.04.013

(18). Ruoslahti E The RGD Story: A Personal Account. 2003, 22, 459–465. 10.1016/S0945-053X

(19). Sharma S; Floren M; Ding Y; Stenmark KR; Tan W; Bryant SJ A Photoclickable Peptide Microarray Platform for Facile and Rapid Screening of 3-D Tissue Microenvironments. Biomaterials 2017, 143, 17–28. 10.1016/j.biomaterials.2017.07.025 [PubMed: 28756193]

(20). Rehmann MS; Luna JI; Maverakis E; Kloxin AM Tuning Microenvironment Modulus and Biochemical Composition Promotes Human Mesenchymal Stem Cell Tenogenic Differentiation. J. Biomed. Mater. Res. A 2016, 104 (5), 1162–1174. 10.1002/jbm.a.35650 [PubMed: 26748903]

(21). Reyes CD; García AJ Engineering Integrin-Specific Surfaces with a Triple-Helical Collagen-Mimetic Peptide. J. Biomed. Mater. Res. A 2003, 65 (4), 511–523. 10.1002/jbm.a.10550 [PubMed: 12761842]

(22). Hennessy KM; Pollot BE; Clem WC; Phipps MC; Sawyer AA; Culpepper BK; Bellis SL The Effect of Collagen I Mimetic Peptides on Mesenchymal Stem Cell Adhesion and Differentiation, and on Bone Formation at Hydroxyapatite Surfaces. Biomaterials 2009, 30 (10), 1898–1909. 10.1016/j.biomaterials.2008.12.053 [PubMed: 19157536]

(23). Gould ST; Darling NJ; Anseth KS Small Peptide Functionalized Thiol-Ene Hydrogels as Culture Substrates for Understanding Valvular Interstitial Cell Activation and de Novo Tissue Deposition. Acta Biomater 2012, 8 (9), 3201–3209. 10.1016/j.actbio.2012.05.009 [PubMed: 22609448]

(24). Hynd MR; Frampton JP; Dowell-Mesfin N; Turner JN; Shain W Directed Cell Growth on Protein-Functionalized Hydrogel Surfaces. J. Neurosci. Methods 2007, 162 (1–2), 255–263. 10.1016/j.jneumeth.2007.01.024 [PubMed: 17368788]

(25). Gould ST; Anseth KS Role of Cell – Matrix Interactions on VIC Phenotype and Tissue Deposition in 3D PEG Hydrogels. J. Tissue Eng. Regen. Med 2013, 10 (10), E443–E543. 10.1002/term.1836 [PubMed: 24130082]

(26). Mabry KM; Schroeder ME; Payne SZ; Anseth KS Three-Dimensional High-Throughput Cell Encapsulation Platform to Study Changes in Cell-Matrix Interactions. ACS Appl. Mater. Interfaces 2016, 8 (34), 21914–21922. 10.1021/acsami.5b11359 [PubMed: 27050338]

(27). Ochsenhirt SE; Kokkoli E; McCarthy JB; Tirrell M Effect of RGD Secondary Structure and the Synergy Site PHSRN on Cell Adhesion, Spreading and Specific Integrin Engagement. Biomaterials 2006, 27 (20), 3863–3874. 10.1016/j.biomaterials.2005.12.012 [PubMed: 16563498]

(28). Reyes CD; García AJ Alpha2beta1 Integrin-Specific Collagen-Mimetic Surfaces Supporting Osteoblastic Differentiation. J. Biomed. Mater. Res. A 2004, 69 (4), 591–600. 10.1002/jbm.a.30034 [PubMed: 15162400]

(29). Hinz B; Phan SH; Thannickal VJ; Prunotto M; Desmoulière A; Varga J; De Wever O; Mareel M; Gabbiani G Recent Developments in Myofibroblast Biology: Paradigms for Connective Tissue Remodeling. Am. J. Pathol 2012, 180 (4), 1340–1355. 10.1016/j.ajpath.2012.02.004 [PubMed: 22387320]

(30). Fairbanks BD; Schwartz MP; Halevi AE; Nuttelman CR; Bowman CN; Anseth KS A Versatile Synthetic Extracellular Matrix Mimic via Thiol-Norbornene Photopolymerization. Adv. Mater 2009, 21 (48), 5005–5010. 10.1002/adma.200901808.A [PubMed: 25377720]

(31). Fairbanks BD; Schwartz MP; Bowman CN; Anseth KS Photoinitiated Polymerization of PEG-Diacrylate with Lithium Phenyl-2,4,6-Trimethylbenzoylphosphinate: Polymerization Rate and Cytocompatibility. Biomaterials 2009, 30 (35), 6702–6707. 10.1016/j.biomaterials.2009.08.055 [PubMed: 19783300]

(32). Kloxin AM; Kasko AM; Salinas CN; Anseth KS Photodegradable Hydrogels for Dynamic Tuning of Physical and Chemical Properties. Science 2009, 324 (5923), 59–63. 10.1126/science.1169494 [PubMed: 19342581]

(33). Rehmann MS; Luna JI; Maverakis E; Kloxin AM Tuning Microenvironment Modulus and Biochemical Composition Promotes Human Mesenchymal Stem Cell Tenogenic Differentiation. J. Biomed. Mater. Res. Part A 2016, 104A, 1162–1174. 10.1002/jbm.a.35650

(34). DeForest CA; Anseth KS Cytocompatible Click-Based Hydrogels with Dynamically Tunable Properties through Orthogonal Photoconjugation and Photocleavage Reactions. Nat. Chem 2011, 3 (12), 925–931. 10.1038/nchem.1174 [PubMed: 22109271]

(35). Balestrini JL; Chaudhry S; Sarrazy V; Koehler A; Hinz B The Mechanical Memory of Lung Myofibroblasts. Integr. Biol. (Camb) 2012, 4 (4), 410–421. 10.1039/c2ib00149g [PubMed: 22410748]

(36). Wang H; Tibbitt MW; Langer SJ; Leinwand LA; Anseth KS Hydrogels Preserve Native Phenotypes of Valvular Fibroblasts through an Elasticity-Regulated PI3K/AKT Pathway. Proc. Natl. Acad. Sci. U. S. A 2013, 11 (48), 19336–19341. 10.1073/pnas.1306369110/-/DC

(37). Ma H; Killaars AR; DelRio FW; Yang C; Anseth KS Myofibroblastic Activation of Valvular Interstitial Cells Is Modulated by Spatial Variations in Matrix Elasticity and Its Organization. Biomaterials 2017, 131, 131–144. 10.1016/j.biomaterials.2017.03.040 [PubMed: 28390245]

(38). Fairbanks BD; Schwartz MP; Halevi AE A Versatile Synthetic Extracellular Matrix Mimic via Thiol-Norbornene Photopolymerization. Adv. Mater 2014, 21 (48), 5005–5010. 10.1002/adma.200901808

(39). Tibbitt MW; Kloxin AM; Sawicki L; Anseth KS Mechanical Properties and Degradation of Chain and Step Polymerized Photodegradable Hydrogels. Macromolecules 2013, 46 (7). 10.1021/ma302522x

(40). Booth AJ; Hadley R; Cornett AM; Dreffs AA; Mattes SA; Tsui JL; Weiss K; Horowitz JC; Fiore VF; Barker TH; et al. Acellular Normal and Fibrotic Human Lung Matrices as a Culture System for In Vitro Investigation. Am. J. Respir. Crit. Care Med 2012, 186 (9), 866–876. 10.1164/rccm.201204-0754OC [PubMed: 22936357]

(41). Huang X; Yang N; Fiore VF; Barker TH; Sun Y; Morris SW; Ding Q; Thannickal VJ; Zhou Y Matrix Stiffness-Induced Myofibroblast Differentiation Is Mediated by Intrinsic Mechanotransduction. Am. J. Respir. Cell Mol. Biol 2012, 47 (3), 340–348. 10.1165/rcmb.2012-0050OC [PubMed: 22461426]

(42). Wen JH; Vincent LG; Fuhrmann A; Choi YS; Hribar KC; Taylor-Weiner H; Chen S; Engler AJ Interplay of Matrix Stiffness and Protein Tethering in Stem Cell Differentiation. Nat. Mater 2014, 13, 1–21. 10.1038/nmat4051 [PubMed: 24343503]

(43). Kloxin AM; Benton JA; Anseth KS In Situ Elasticity Modulation with Dynamic Substrates to Direct Cell Phenotype. Biomaterials 2010, 31 (1), 1–8. 10.1016/j.biomaterials.2009.09.025 [PubMed: 19788947]

(44). Weber LM; Anseth KS Hydrogel Encapsulation Environments Functionalized with Extracellular Matrix Interactions Increase Islet Insulin Secretion. Matrix Biol 2008, 27 (8), 667–673. 10.1016/j.matbio.2008.08. [PubMed: 18773957]

(45). Lee Y-H; Huang J-R; Wang Y-K; Lin K-H Three-Dimensional Fibroblast Morphology on Compliant Substrates of Controlled Negative Curvature. Integr. Biol. (Camb) 2013, 5 (12), 1447–1455. 10.1039/c3ib40161h [PubMed: 24132182]

(46). Dubey G; Mequanint K Conjugation of Fibronectin onto Three-Dimensional Porous Scaffolds for Vascular Tissue Engineering Applications. Acta Biomater 2011, 7 (3), 1114–1125. 10.1016/j.actbio.2010.11.010 [PubMed: 21073985]

(47). Masters KS; Shah DN; Walker G; Leinwand LA; Anseth KS Designing Scaffolds for Valvular Interstitial Cells: Cell Adhesion and Function on Naturally Derived Materials. J. Biomed. Mater. Res. A 2004, 71 (1), 172–180. 10.1002/jbm.a.30149 [PubMed: 15368267]

(48). Hinz B; Gabbiani G Cell-Matrix and Cell-Cell Contacts of Myofibroblasts: Role in Connective Tissue Remodeling. Thromb. Haemost 2003, 90 (6), 993–1002. 10.1160/TH03-05-0328 [PubMed: 14652629]

(49). Wang H; Haeger SM; Kloxin AM; Leinwand LA; Anseth KS Redirecting Valvular Myofibroblasts into Dormant Fibroblasts through Light-Mediated Reduction in Substrate Modulus. PLoS One 2012, 7 (7), e39969 10.1371/journal.pone.0039969 [PubMed: 22808079]

(50). Chia HN; Vigen M; Kasko AM Effect of Substrate Stiffness on Pulmonary Fibroblast Activation by TGF-B. Acta Biomater 2012, 8 (7), 2602–2611. 10.1016/j.actbio.2012.03.027 [PubMed: 22446029]

(51). Serini G; Bochaton-Piallat ML; Ropraz P; Geinoz A; Borsi L; Zardi L; Gabbiani G The Fibronectin Domain ED-A Is Crucial for Myofibroblastic Phenotype Induction by Transforming Growth Factor-beta1. J. Cell Biol 1998, 142 (3), 873–881. 10.1083/jcb.142.3.873 [PubMed: 9700173]

(52). Muro AF; Moretti FA; Moore BB; Yan M; Atrasz RG; Wilke CA; Flaherty KR; Martinez FJ; Tsui JL; Sheppard D; et al. An Essential Role for Fibronectin Extra Type III Domain A in Pulmonary Fibrosis. Am. J. Respir. Crit. Care Med 2008, 177 (6), 638–645. 10.1164/rccm.200708-1291OC [PubMed: 18096707]

(53). Jones MG; Fabre A; Schneider P; Cinetto F; Sgalla G; Mavrogordato M; Jogai S; Alzetani A; Marshall BG; O'Reilly KMA; et al. Three-Dimensional Characterization of Fibroblast Foci in Idiopathic Pulmonary Fibrosis. JCI Insight 2016, 1 (5), 1–11. 10.1172/jci.insight.86375

(54). Crouch E Pathobiology of Pulmonary Fibrosis. Am. J. Physiol 1990, 259 (4 Pt 1), L159–84. 10.1152/ajplung.1990.259.4.L159 [PubMed: 2221080]

(55). Yamamoto M; Yamato M; Aoyagi M; Yamamoto K Identification of Integrins Involved in Cell Adhesion to Native and Denatured Type I Collagens and the Phenotypic Transition of Rabbit Arterial Smooth Muscle Cells. Exp Cell Res 1995, pp 249–256. 10.1006/excr.1995.1225

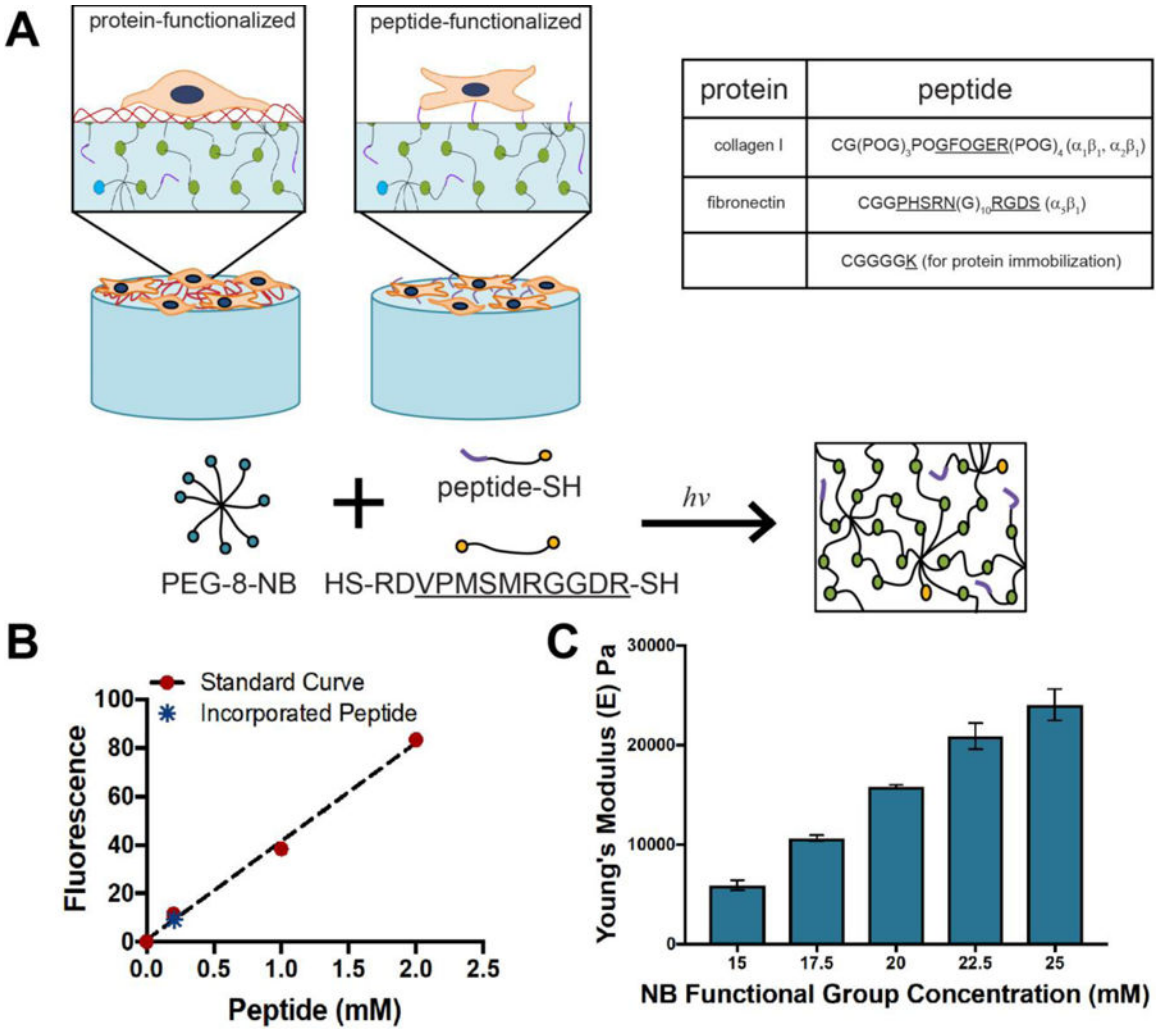

Figure 1. Synthetic matrix design for comparing cell response to hydrogels that were — formed by step growth polymerization and functionalized with proteins and integrin-binding peptides.

A) Eight-arm PEG-norbornene was reacted with a di-thiol MMP-degradable peptide (GCRDVPMS↓MRGGDRCG) in the presence of LAP and 365 nm light to form a step-growth hydrogel network. This mechanism of network formation allows the incorporation of different thiol-presenting peptide sequences for promoting cell binding or presenting of amines for subsequent immobilization of whole ECM proteins, as summarized in the table. **B)** Using a fluorescently-labeled model peptide (CGRGDS-AF488), the concentration of pendant peptide incorporated into the hydrogel network was observed to be approximately 0.25 mM at equilibrium swelling. **C)** By altering the weight percent of total monomer in the system (1:1 NB:SH), various moduli can be achieved. For all cell culture studies, the composition of 20 mM NB was selected as it results in a matrix modulus known to promote fibroblast activation, specifically E ~ 15 kPa, allowing examination of any differences in activation in response to the selected ECM proteins and their peptide mimics.

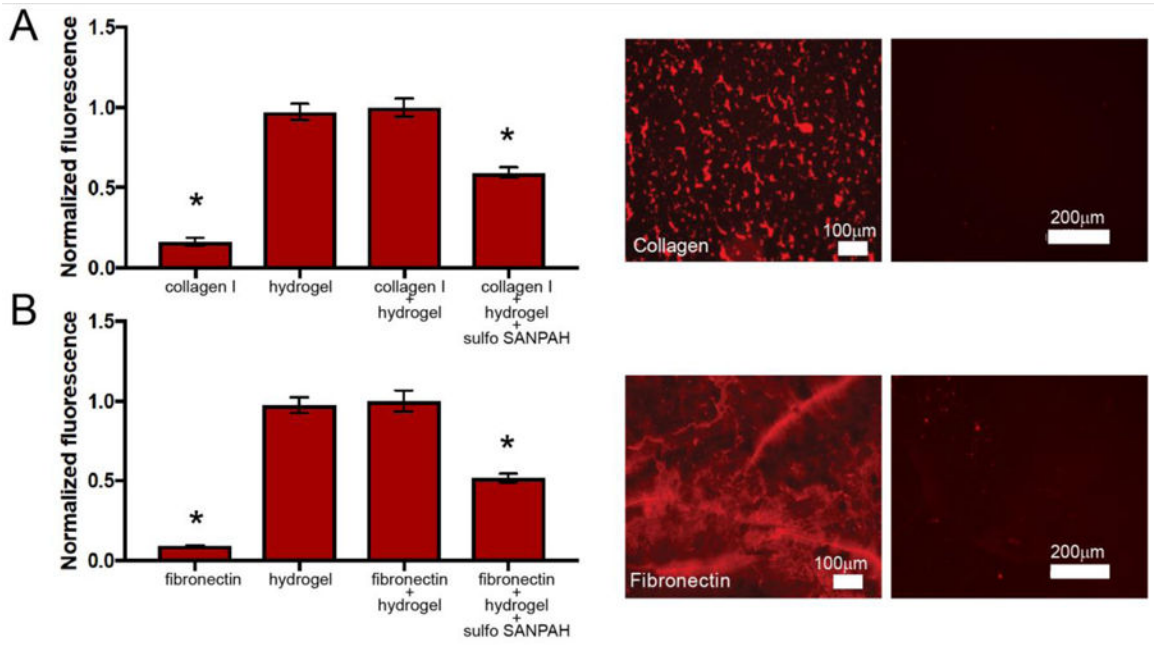

Figure 2. Functionalization of hydrogels with whole ECM proteins.

Collagen I and fibronectin were conjugated to the surface of step-growth hydrogels using Sulfo-SANPAH chemistry. For both proteins, a semi-quantitative fluorescence based assay was used to assess the consumption of amines upon conjugation, and separately, presentation of the protein on the surface of hydrogels was qualitatively assessed by microscopy. First, to assess consumption of amines upon reaction with Sulfo-SANPAH, fluoraldehyde-OPA solution was added to whole protein solution, amine-functionalized polymerized hydrogel, hydrogel and whole protein solution, and hydrogel and whole protein solution that was treated with Sulfo-SANPAH. Fluoraldehyde-OPA reacts with free primary amines to create a fluorescent product, such that fluorescence correlates directly with amine concentration in the sample. For both **A)** collagen I (graph) and **B)** fibronectin (graph), we observed a decrease in fluorescence when Sulfo-SANPAH was used to conjugate each respective whole proteins to the surface of the PEG hydrogels, indicating that primary amines had been consumed in the conjugation reaction (* $p < 0.05$). Further, immunofluorescent labeling was used to visualize protein on the surface of the hydrogels. **A)** Collagen I (left image) and **B)** fibronectin (left image) were observed on the surface of Sulfo-SANPAH treated hydrogels using immunostaining and epifluorescence microscopy, whereas little background was observed upon staining of control samples where hydrogels had been incubated with the respective protein without Sulfo-SANPAH conjugation (right images).

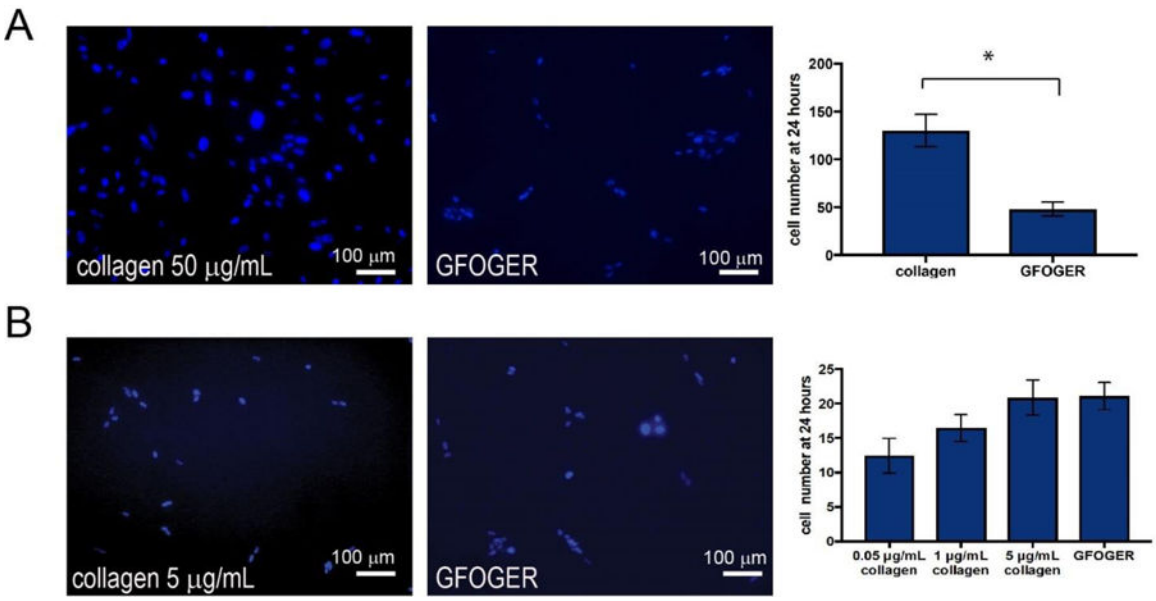

Figure 3. Examination of different substrate compositions for achieving uniform cell attachment between collagen I and GFOGER.

A) Human pulmonary fibroblasts were seeded on hydrogels functionalized with 50 μg/mL collagen I or GFOGER peptide, and initial cell attachment assessed (24 hours), staining cell nuclei (Hoescht, blue) and counting number of cells per field of view. Cell attachment to hydrogels containing 50 μg/mL collagen I was observed to be higher than attachment to hydrogels containing the GFOGER peptide (*$p<0.05$). **B)** To identify a collagen concentration that resulted in uniform initial cell-cell contact on protein- and peptide-functionalized substrates, cells were seeded on hydrogels functionalized with a range of collagen I concentrations (0.05 μg/mL to 5 μg/mL). A collagen I concentraiton of 5 μg/mL was identified to produce the most similar cell attachment to that observed with GFOGER.

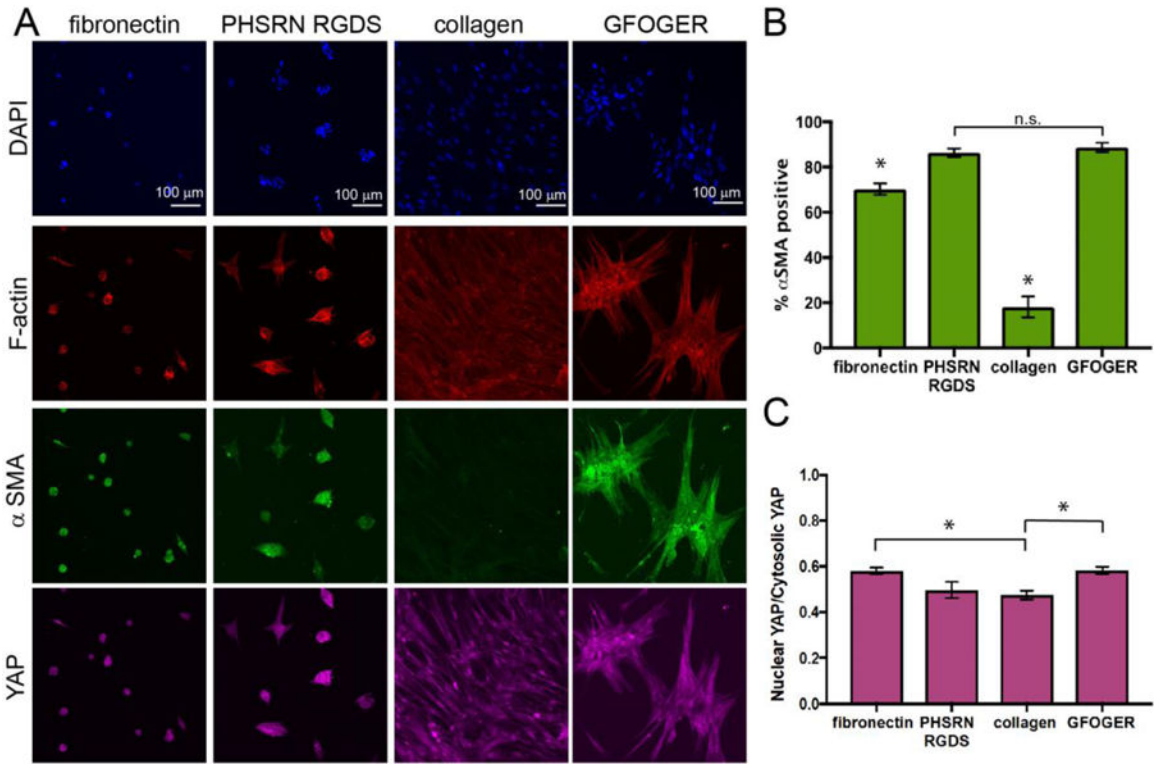

Figure 4. Fibroblast activation on protein- and peptide-functionalized hydrogels.

A) Human pulmonary fibroblasts were cultured on hydrogels functionalized with fibronectin, PHSRN-RGDS, collagen I, or GFOGER. Cell morphology and activation were assessed 72 hours after seeding immunostaining (F-actin (red), αSMA (green), YAP (pink), and DAPI for nuclei (blue)). **B)** Significantly more αSMA positive fibroblasts were observed on GFOGER- and PHSRN-RGDS-functionalized hydrogels relative to substrates functionalized with their whole-protein counterparts of collagen and fibronectin, respectively (*$p<0.01$). **C)** YAP nuclear localization was determined by measuring fluorescence intensity in the nuclei (nuclear YAP) and dividing it by fluorescence intensity in the cytoplasm (cytosolic YAP), where YAP localization is correlated with fibroblast activation. Fibroblasts cultured on collagen I-functionalized hydrogels displayed significantly less YAP nuclear localization than fibroblasts cultured on GFOGER-functionalized hydrogels or fibronectin-functionalized hydrogels (*$p < 0.05$). Taken together, these data suggest increased activation of fibroblasts on peptide-functionalized substrates, with significantly increased activation on GFOGER- relative to collagen I-functionalized substrates.

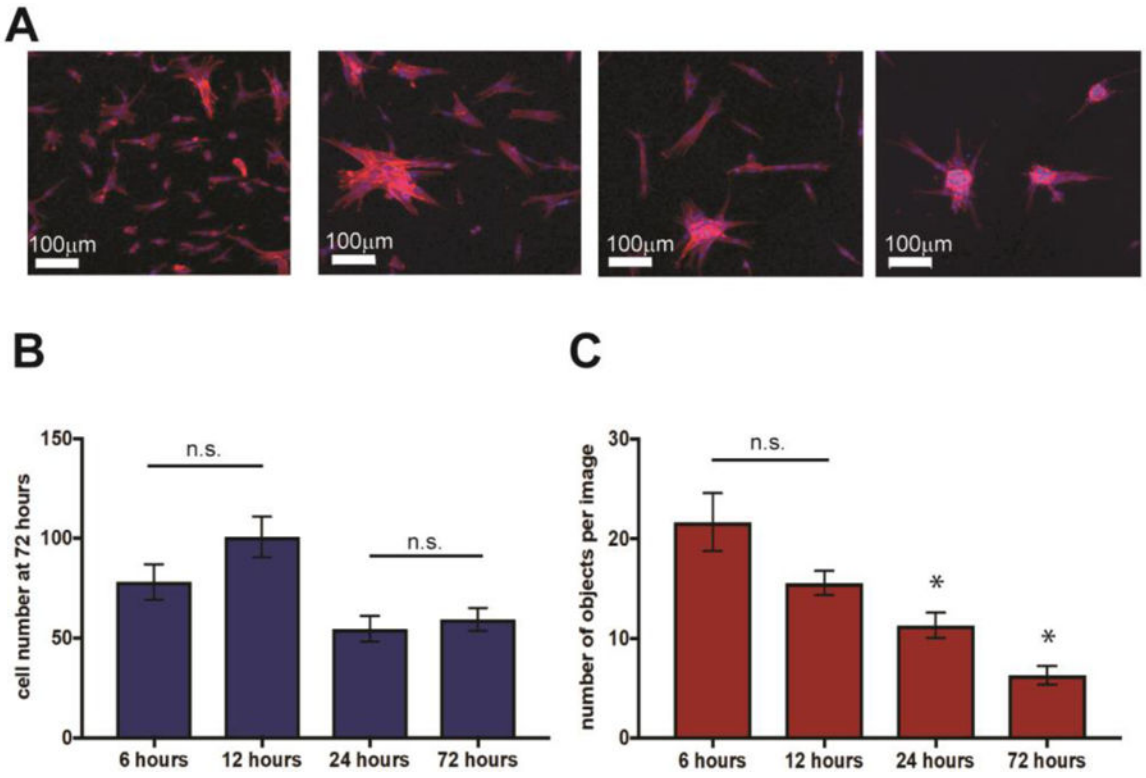

Figure 5. Fibroblasts form clusters over time on GFOGER-functionalized hydrogels.

A) Human pulmonary fibroblasts (CCL151) were cultured on GFOGER-functionalized hydrogels and fixed and stained with DAPI and for F-actin at both early and later time points to assess initial seeding and subsequent cell response to the synthetic matrix. Qualitatively, cells were observed to form star-shaped clusters over time reminiscent of activated foci that form during lung fibrosis. To more quantitatively assess this, the number of nuclei and the number of objects (individual or clustered cell bodies) were counted. **B)** The total number of cells attached to the substrates was relatively consistent over the time course, with ~ 80 cells per field of view initially and ~ 60 cells per field of view by day 3. **C)** In contrast, the number of objects steadily decreased with time, ~ 20 to ~ 5 per field of view, supporting the formation of clusters of cells and indicative of activation. Number of objects statistically decreased from earlier timepoints at both 24 and 72 hours (* $p<0.05$).

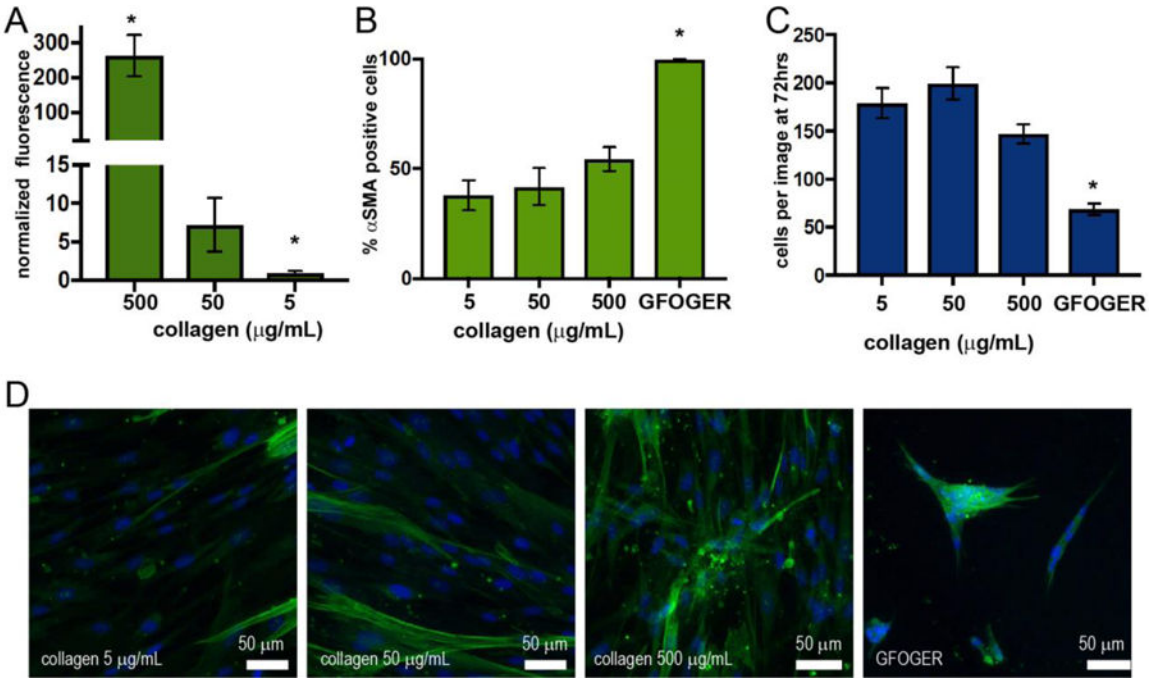

Figure 6. Effects of collagen concentration on fibroblast activation.

Hydrogels were functionalized with different concentrations of collagen I (5 to 500 μg/mL fluorescently-labeled collagen I) using Sulfo-SANPAH chemistry. **A)** where increased fluorescence intensity on hydrogel surfaces was observed with increasing concentrations of collagen using confocal microscopy (* $p < 0.01$). Fibroblasts were seeded on hydrogels with different concentrations of standard (not labeled) collagen and cell response compared to GFOFER-functionalized hydrogels (F-actin (red), αSMA, (green) and with DAPI nuclear stain): **B)** the percentage of αSMA postive cells per image **C)** the number of cells per image, and **D)** representative images. A trend of increasing αSMA positive cells was observed with increasing collagen I concentration; however, the differences between conditions were not statistically signficant, and all collagen conditions were different from GFOGER-functionalized substrates (* $p < 0.01$).